

TASI Lectures on Emergence of Supersymmetry, Gauge Theory and String in Condensed Matter Systems

Sung-Sik Lee^{1,2}

¹Department of Physics & Astronomy, McMaster University,
1280 Main St. W., Hamilton ON L8S4M1, Canada

²Perimeter Institute for Theoretical Physics,
31 Caroline St. N., Waterloo ON N2L2Y5, Canada

Abstract

The lecture note consists of four parts. In the first part, we review a 2+1 dimensional lattice model which realizes emergent supersymmetry at a quantum critical point. The second part is devoted to a phenomenon called fractionalization where gauge boson and fractionalized particles emerge as low energy excitations as a result of strong interactions between gauge neutral particles. In the third part, we discuss about stability and low energy effective theory of a critical spin liquid state where stringy excitations emerge in a large N limit. In the last part, we discuss about an attempt to come up with a prescription to derive holographic theory for general quantum field theory.

Contents

1	Introduction	1
2	Emergent supersymmetry	2
2.1	Emergence of (bosonic) space-time symmetry	3
2.2	Emergent supersymmetry	4
2.2.1	Model	5
2.2.2	RG flow	7
3	Emergent gauge theory	10
3.1	Model	10
3.2	Slave-particle theory	10
3.3	World line picture	12
4	Critical spin liquid with Fermi surface	14
4.1	From spin model to gauge theory	14
4.1.1	Slave-particle approach to spin-liquid states	14
4.1.2	Stability of deconfinement phase in the presence of Fermi surface . . .	16
4.2	Low energy effective theory	17
4.2.1	Failure of a perturbative $1/N$ expansion	20
4.2.2	Genus Expansion	21
5	Holographic description of quantum field theory	25
5.1	Toy-model : 0-dimensional scalar theory	25
5.2	D -dimensional $O(N)$ vector theory	28
5.3	Phase Transition and Critical Behaviors	29
6	Acknowledgment	30

1 Introduction

A variety of phenomena in condensed matter systems ranging from metal to superconductivity can be understood based on simple Hamiltonians, such as the Hubbard model,

$$H = - \sum_{\langle i,j \rangle, \sigma} t_{ij} c_{i\sigma}^\dagger c_{j\sigma} + U \sum_i n_{i\uparrow} n_{i\downarrow} - \mu \sum_i n_i. \quad (1.1)$$

Here t_{ij} , U and μ are hopping integral, on-site Coulomb energy and chemical potential, respectively. $c_{i\sigma}$ is the annihilation operator of electron with spin σ at site i , $n_{i\sigma} = c_{i\sigma}^\dagger c_{i\sigma}$ and $n_i = n_{i\uparrow} + n_{i\downarrow}$. While it is easy to write, it is impossible to solve the Hamiltonian of interacting 10^{23} electrons from the first principle calculation. The symmetry of the Hamiltonian is low and there are few kinematical constraints that simplify dynamics. Because of interactions, one can not in general disentangle a subsystem from the rest to reduce the many-body

problem to one-body problem. Nonetheless, as one probes the system at low energies, various dynamical constraints emerge, which gives us a chance to understand low energy physics by focusing on fewer degrees of freedom. Presumably, the full Hilbert space has a lot of local minima, and the system ‘flows’ to one of the minima in the low energy limit. Around each minimum, the geometrical and topological structures of the low energy manifold determine the nature of low energy degrees of freedom. Quantum fluctuations of the low energy modes are governed by low energy effective theories which are rather insensitive to details of the microscopic Hamiltonian. The distinct set of minima and the associated low energy effective theories characterize different phases of matter (universality classes). One of the goals in condensed matter physics is to classify different phases of matter and understand universal properties of them using low energy effective theories.

Various quantum phases of matter have been identified, such as Landau Fermi liquid, band insulator, superfluid/superconductor, quantum Hall liquid, etc. The list is still growing, and new ways of characterizing different phases are being devised. However, it is likely that there are many new phases yet to be discovered.

There are some interesting aspects we need to appreciate. First, it is usually very hard to predict which phase a given microscopic Hamiltonian flows into. Often, microscopic Hamiltonians do not give much clue over what emerges in the low energy limit. Who could have predicted that the Hubbard model with impurities and defects has superconducting phase where electric current can flow without any resistivity? Second, low energy effective theories in some phases or quantum critical points in condensed matter systems are strikingly similar to what (we believe) describes the very vacuum of our universe [1, 2]. For example, there exists a phase where the low energy effective theory has very high symmetry including supersymmetry even though microscopic Hamiltonian breaks almost all symmetries except for some discrete lattice symmetry and internal global symmetry. In some corner of the landscape, gauge theory emerges as a low energy effective theory of the Hubbard model. In some phases, there is no well-defined quasiparticle. Instead, some weakly coupled stringy excitations emerge as low energy excitations. How is it possible that collective fluctuations of electrons in solids have such striking similarities to the way the vacuum of our own universe fluctuates? Is the universe made of a bunch of non-relativistic ‘electrons’ at very short distance? Perhaps it is simply that there are not too many good ideas that are available to nature, and she has to recycle same ideas in different systems and different scales over and over. In this lecture, we will review a few examples of emergent phenomena in condensed matter systems which are potentially interesting to both condensed matter physicists and high energy physicists.

2 Emergent supersymmetry

In spontaneous symmetry breaking, symmetry of microscopic model is broken at low energies as the ground state spontaneously choose a particular vacuum among degenerate vacua connected by the symmetry. In condensed matter systems, the opposite situation often arises. Namely, new symmetry which is absent in microscopic Hamiltonian can arise at low energies as the system dynamically organizes itself to show a pattern of fluctuations which obey certain symmetry in the long distance limit. Sometimes, gapless excitations (or ground

state degeneracy) whose origins are not obvious from any microscopic symmetry can be protected by emergent symmetries.

2.1 Emergence of (bosonic) space-time symmetry

Consider a rotor model in one-dimensional lattice,

$$H_b = -t \sum_i (e^{i(\theta_i - \theta_{i+1})} + h.c.) + \frac{U}{2} \sum_i (n_i - \bar{n})^2, \quad (2.1)$$

where θ_i (n_i) is phase (number) of bosons at site i which satisfies $[\theta_i, n_j] = i\delta_{ij}$, and \bar{n} is the average density. For integer \bar{n} , the long distance physics is captured by the 1+1D XY model

$$S = \kappa \int dx^2 (\partial_\mu \theta)^2, \quad (2.2)$$

where $\kappa \sim \sqrt{t/U}$. Because θ is compact, instanton is allowed where the winding number

$$\nu(t) = \int_0^L dx \partial_x \theta(t, x) \quad (2.3)$$

changes by an integer multiple of 2π . Here we consider the periodic boundary condition : $e^{i\theta(t,0)} = e^{i\theta(t,L)}$. Physically, a unit instanton describes quantum tunneling from a state with momentum k to a state with momentum $k + 2\bar{n}\pi/a$ with a the lattice spacing. This tunneling is allowed because momentum needs to be conserved only modulo $2\pi/a$ due to the underlying lattice.¹

If $\kappa \gg 1$, instantons are dynamically suppressed even though no microscopic symmetry prevents them. In this case, the absolute value of momentum is conserved, not just in modulo $2\pi/a$. Since the state with momentum $2\bar{n}\pi/a$ does not mix with the state with zero momentum, states with non-trivial windings arise as well-defined excitations which becomes gapless excitation in the thermodynamic limit. Note that this gapless excitation is not a Goldstone mode because the continuous symmetry can not be broken in 1+1D even at $T = 0$. This gapless mode is a topological excitation protected by the emergent conservation law. Within each topological sector, we can treat θ as a non-compact variable and the low energy theory becomes a free theory.

If $\kappa \ll 1$, the potential energy dominates and bosons are localized, exhibiting gap. In terms of the XY-model, instantons and anti-instantons proliferate, and the system can not ignore the existence of lattice anymore.

Now let's consider a simple two-dimensional lattice model where rotational symmetry emerges,

$$H_b = -t \sum_{\langle i,j \rangle} (b_i^\dagger b_j + h.c.) - \mu \sum_i b_i^\dagger b_i, \quad (2.4)$$

¹In the T-dual variable $\partial_\mu \phi = \epsilon_{\mu\nu} \partial_\nu \theta$, the non-conservation of the winding number translates into the (explicitly) broken translational symmetry in the target space ϕ , and the theory is mapped into the sine-Gordon model.

where t is the hopping energy, μ is chemical potential, and $\langle i, j \rangle$ denotes nearest neighbor sites on the square lattice. The energy spectrum is given by

$$E_k = -2t(\cos k_x + \cos k_y) - \mu. \quad (2.5)$$

The full spectrum respects only the 90 degree rotational symmetry. If the chemical potential is tuned to the bottom of the band, the energy dispersion of low energy bosons become

$$E_k = tk^2 + O(k^4). \quad (2.6)$$

In the low energy limit, higher order terms are irrelevant and the full rotational symmetry emerges.

Besides the rotational symmetry, the full Lorentz symmetry can emerge. For example, the low energy excitations of fermions at half filling on the honeycomb lattice are described by two copies of two-component Dirac fermions in 2+1 dimensions. As a result, the full Lorentz symmetry emerges in the low energy limit although the microscopic model has only six-fold rotational symmetry. When there are gapless excitations in the presence of Lorentz symmetry, usually the full conformal symmetry is realized.

2.2 Emergent supersymmetry

Supersymmetry is a symmetry which relates bosons and fermions. Since bosons and fermions have integer and half integer spins respectively in relativistic systems, supercharges that map boson into fermion (or vice versa) carry half integer spin and supersymmetry should be a part of space-time symmetry. Moreover, supersymmetry is the unique non-trivial extension of the Poincare symmetry besides the conformal symmetry. Given that all bosonic space-time symmetry can emerge in condensed matter systems, one can ask whether supersymmetry can also emerge ².

In 2D, it is known that supersymmetry can emerge from the dilute Ising model [3],

$$\beta H = -J \sum_{\langle i, j \rangle} \sigma_i \sigma_j - \mu \sum_i \sigma_i^2, \quad (2.7)$$

where $\sigma = \pm 1$ represents a site with spin up or down, and $\sigma = 0$ represents a vacant site. When μ is large, almost all sites are filled and the usual second order Ising transition occurs as J is tuned. As μ is lowered, the second order transition terminates at a tricritical point $\mu = \mu_c$ and the phase transition becomes first order below μ_c . The tricritical point is described by the Φ^6 -theory,

$$S = \int d^2x [(\partial_\mu \Phi)^2 + \lambda_6 \Phi^6] \quad (2.8)$$

where $\Phi \sim \langle \sigma \rangle$ describes the magnetic order parameter. Although there is no fermion in this action, one can construct a fermion field ψ from a string of spins through the Jordan-Wigner transformation. At the tricritical point, the scaling dimensions of Φ^2 and ψ differ

² There are large literatures on supersymmetric quantum mechanics in condensed matter systems. Here we will exclusively focus on full space-time supersymmetry.

exactly by 1/2. This is not an accident and these two fields form a multiplet under an emergent supersymmetry. More generally, the operators which are even (odd) under the Z_2 spin symmetry form the Neveu-Schwarz (Ramond) algebra. The dilute Ising model provides deformations of the underlying superconformal theory within $(-1)^F = 1$ sector, where F is the fermion number. For lattice realizations of other 2D superconformal field theories, see Ref. [6, 7].

To realize emergent supersymmetry in higher dimensions, it is desired to have an interacting theory in the IR limit [4]. Otherwise, RG flow of supersymmetry-breaking couplings would stop below certain energy scale, and supersymmetry-breaking terms generically survive in the IR limit. It is hard to have free bosons and fermions which have same velocity unless enforced by some exact microscopic symmetry. In this sense, 2+1D is a good (but not exclusive) place to look for an emergent supersymmetry. In 3+1D, it has been suggested that the $\mathcal{N} = 1$ super Yang-Mills theory can emerge from a model of gauge boson and chiral fermion in the adjoint representation [5].³ If a subset of supersymmetry is kept as exact symmetry in lattice models, a full supersymmetry can emerge in the continuum [8]. Here, we will consider a 2+1D lattice model where supersymmetry dynamically emerge at a critical point without any lattice supersymmetry [9].

2.2.1 Model

The Hamiltonian is composed of three parts,

$$H = H_f + H_b + H_{fb}, \quad (2.9)$$

where

$$\begin{aligned} H_f &= -t_f \sum_{\langle i,j \rangle} (f_i^\dagger f_j + h.c.), \\ H_b &= t_b \sum_{\langle I,J \rangle} (e^{i(\theta_I - \theta_J)} + h.c.) + \frac{U}{2} \sum_I n_I^2, \\ H_{fb} &= h_0 \sum_I e^{i\theta_I} (f_{I+\mathbf{b}_1} f_{I-\mathbf{b}_1} + f_{I-\mathbf{b}_2} f_{I+\mathbf{b}_2} + \\ &\quad + f_{I-\mathbf{b}_1+\mathbf{b}_2} f_{I+\mathbf{b}_1-\mathbf{b}_2}) + h.c.. \end{aligned} \quad (2.10)$$

Here H_f describes spinless fermions with nearest neighbor hopping on the honeycomb lattice at half filling; H_b describes bosons with nearest neighbor hopping and an on-site repulsion on the triangular lattice which is dual to the honeycomb lattice; and H_{fb} couples the fermions and bosons. The lattice structure is shown in Fig. 1 (a). f_i is the fermion annihilation operator and $e^{-i\theta_I}$, the lowering operator of n_I which is conjugate to the angular variable θ_I . $\langle i, j \rangle$ and $\langle I, J \rangle$ denote pairs of nearest neighbor sites on the honeycomb and triangular lattices, respectively. $t_f, t_b > 0$ are the hopping energies for the fermions and bosons,

³But the notion of emergent supersymmetry is less sharp in this case due to the fact that confinement sets in below an energy scale and there is no genuine IR degrees of freedom. For a given gauge coupling at the lattice scale, supersymmetry is realized as an approximate symmetry between fermionic and bosonic glue ball spectra.

respectively and U is the on-site boson repulsion energy. \mathbf{b}_1 and \mathbf{b}_2 are two independent vectors which connect a site on the triangular lattice to the neighboring honeycomb lattice sites. h_0 is the pairing interaction strength associated with the process where two fermions in the f-wave channel around a hexagon are paired and become a boson at the center of the hexagon, and vice versa. In this sense, the boson can be regarded as a Cooper pair made of two spinless fermions in the f-wave wavefunction. This model has a global U(1) symmetry under which the fields transform as $f_i \rightarrow f_i e^{i\varphi}$ and $e^{-i\theta_I} \rightarrow e^{-i\theta_I} e^{i2\varphi}$.

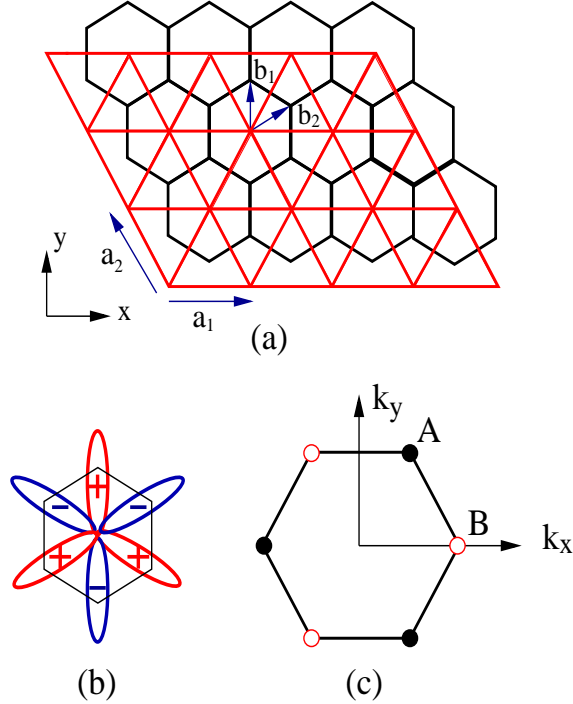


Figure 1: (a) The lattice structure in the real space. Fermions are defined on the honeycomb lattice and the bosons, on the dual triangular lattice. \mathbf{a}_1 , \mathbf{a}_2 are the lattice vectors with length a , and \mathbf{b}_1 , \mathbf{b}_2 , two independent vectors which connect a site on the triangular lattice to the nearest neighbor sites on the honeycomb lattice. (b) The phases of a fermion pair in the real space. (c) The first Brillouin zone in the momentum space. A and B indicate two inequivalent points with momenta $\mathbf{k}_A = \frac{2\pi}{a}(\frac{1}{3}, \frac{1}{\sqrt{3}})$ and $\mathbf{k}_B = \frac{2\pi}{a}(\frac{2}{3}, 0)$ where the low energy modes are located. ψ_1, ϕ_2 are located at \mathbf{k}_A and ψ_2, ϕ_1 , at \mathbf{k}_B .

In the low energy limit, there are two copies of Dirac fermions and two complex bosons. One set of Dirac fermion and complex boson carries momentum \mathbf{k}_A , and the other set carries momentum \mathbf{k}_B . The fermions are massless without any fine tuning, which is protected by the time reversal symmetry and the inversion symmetry. The reason why we have two complex bosons instead of one is that the boson kinetic energy is frustrated. Because $t_b > 0$, the boson kinetic energy is minimized when relative phases between neighboring bosons become π . However, not all kinetic energy terms can be minimized due to the geometrical

frustration of the triangular lattice where bosons are defined. The best thing the bosons can do to minimize the kinetic energy is to form a ‘spiral wave’ where the phase of bosons rotates either by 120 or -120 degree around triangles. There are two such global configurations and they carry the momenta \mathbf{k}_A and \mathbf{k}_B respectively. Each complex boson describes condensate of bosons in each of these configurations. The effective theory for the low energy modes becomes

$$\begin{aligned}
\mathcal{L} = & i \sum_{n=1}^2 \bar{\psi}_n \left(\gamma_0 \partial_\tau + c_f \sum_{i=1}^2 \gamma_i \partial_i \right) \psi_n \\
& + \sum_{n=1}^2 \left[|\partial_\tau \phi_n|^2 + c_b^2 \sum_{i=1}^2 |\partial_i \phi_n|^2 + m^2 |\phi_n|^2 \right] \\
& + \lambda_1 \sum_{n=1}^2 |\phi_n|^4 + \lambda_2 |\phi_1|^2 |\phi_2|^2 \\
& + h \sum_{n=1}^2 (\phi_n^* \psi_n^T \varepsilon \psi_n + c.c.). \tag{2.11}
\end{aligned}$$

A closely related field theory has been studied in the context of high T_c superconductors [11]. Although there are same number of propagating bosons and fermions⁴, this Lagrangian contains four supersymmetry breaking terms,

$$\begin{aligned}
m & \neq 0, \\
c_b & \neq c_f, \\
\lambda_1 & \neq h^2, \\
\lambda_2 & \neq 0. \tag{2.12}
\end{aligned}$$

One would naively expect that one has to tune at least four parameters to reach the supersymmetric point. However, it turns out that one needs to tune only the boson mass to realize supersymmetry.

2.2.2 RG flow

To control the theory, we consider the theory in $4 - \epsilon$ dimensions. We use the dimensional regularization scheme where the number of fermion components and the traces of gamma matrices are fixed.

The boson mass is a relevant (supersymmetry-breaking) perturbation and we tune it (by hand) to zero. This amounts to tuning one microscopic parameter to reach the critical point which separates the normal phase and the bose condensed phase. The one-loop beta

⁴One complex boson is worthy of two components of complex fermions in terms of the number of initial data one has to specify to solve the equation of motion.

functions for the remaining couplings at the critical point is given by

$$\begin{aligned}
\frac{dh}{dl} &= \frac{\epsilon}{2}h - \frac{1}{(4\pi c_f)^2} \left(2 + \frac{16c_f^3}{c_b(c_f + c_b)^2} \right) h^3, \\
\frac{d\lambda_1}{dl} &= \epsilon\lambda_1 - \frac{1}{(4\pi)^2} \left(\frac{20\lambda_1^2 + \lambda_2^2}{c_b^2} + \frac{8h^2\lambda_1}{c_f^2} - \frac{16h^4}{c_f^2} \right), \\
\frac{d\lambda_2}{dl} &= \epsilon\lambda_2 - \frac{1}{(4\pi)^2} \left(\frac{4\lambda_2^2 + 16\lambda_1\lambda_2}{c_b^2} + \frac{8h^2\lambda_2}{c_f^2} \right), \\
\frac{dc_f}{dl} &= \frac{32h^2c_f(c_b - c_f)}{3(4\pi)^2c_b(c_b + c_f)^2}, \\
\frac{dc_b}{dl} &= -\frac{2h^2c_b(c_b^2 - c_f^2)}{(4\pi c_b c_f)^2},
\end{aligned} \tag{2.13}$$

where the logarithmic scaling parameter l increases in the infrared. The RG flow is shown in Fig. 2.

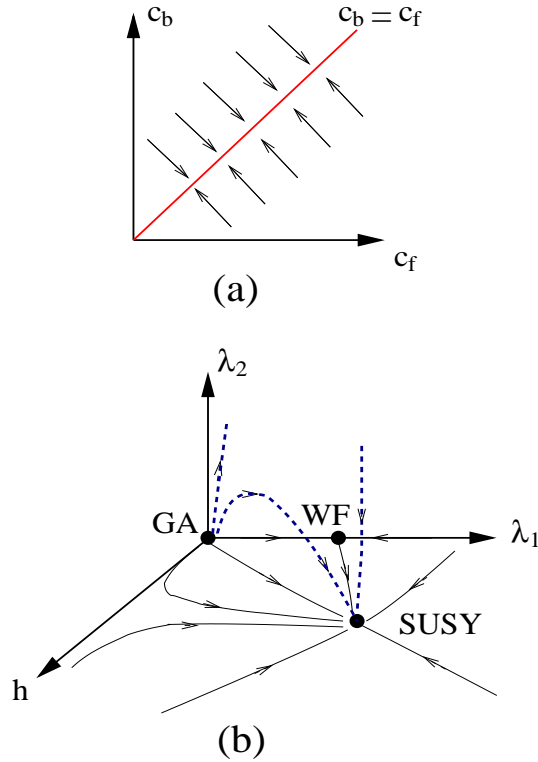


Figure 2: The schematic RG flows of (a) the velocities with $h \neq 0$ and (b) λ_1 , λ_2 and h in the subspace of $m = 0$. In (b), the solid lines represent the flow in the plane of (h, λ_1) and the dashed lines, the flow outside the plane.

The Gaussian (GA) fixed point, $(h^*, \lambda_1^*, \lambda_2^*) = (0, 0, 0)$, the Wilson-Fisher (WF) fixed point, $(h^*, \lambda_1^*, \lambda_2^*) = (0, \frac{(4\pi c_b)^2 \epsilon}{20}, 0)$, and the $O(4)$ fixed point, $(h^*, \lambda_1^*, \lambda_2^*) = (0, \frac{(4\pi c_b)^2 \epsilon}{24}, \frac{(4\pi c_b)^2 \epsilon}{12})$ are all unstable upon turning on the pairing interaction h . If h is nonzero, the boson and

fermion velocities begin to flow as can be seen from the last two equations in Eq. (2.13). Because the pairing interaction mixes the velocities of the boson and fermion, the difference of the velocities exponentially flows to zero in the low-energy limit. The converged velocity in the infrared limit is a non-universal value which we will scale to 1 in the followings. With a nonzero h , the system eventually flows to a stable fixed point,

$$(h^*, \lambda_1^*, \lambda_2^*) = \left(\sqrt{\frac{(4\pi)^2 \epsilon}{12}}, \frac{(4\pi)^2 \epsilon}{12}, 0 \right). \quad (2.14)$$

At this point, the theory becomes invariant under the supersymmetry transformation,

$$\begin{aligned} \delta_\xi \phi_n &= -\bar{\psi}_n \xi, & \delta_\xi \phi_n^* &= \bar{\xi} \psi_n \\ \delta_\xi \psi_n &= i \not{\partial} \phi_n^* \xi - \frac{h}{2} \phi_n^2 \varepsilon \bar{\xi}^T, & \delta_\xi \bar{\psi}_n &= i \bar{\xi} \not{\partial} \phi_n - \frac{h}{2} \phi_n^{*2} \xi^T \varepsilon, \end{aligned} \quad (2.15)$$

where ξ is a two-component complex spinor. This theory corresponds to the $\mathcal{N} = 2$ (which amounts to four supercharges) Wess-Zumino model with superpotential,

$$F = \frac{h}{3} (\Phi_1^3 + \Phi_2^3), \quad (2.16)$$

where Φ_1 and Φ_2 are two chiral multiplets. Due to the emergent superconformal symmetry, the one-loop anomalous scaling dimensions for the chiral primary fields ϕ and ψ ,

$$\eta_\phi = \eta_\psi = \epsilon/3 \quad (2.17)$$

are exact.

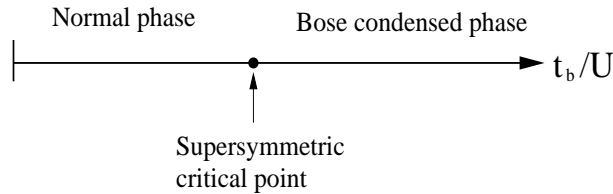


Figure 3: The superconformal theory describes the quantum critical point separating the normal state and the f-wave superconducting (Bose condensed) state of spinless fermions in the honeycomb lattice.

Although the emergent supersymmetry has been obtained from a microscopic model which has both fermions and bosons, one can view bosons as composite particles (Cooper pairs) which emerge at low energies. This implies that supersymmetry can emerge from a microscopic model which contains only fermions. Therefore, the $\mathcal{N} = 2$ Wess-Zumino theory can describe the second order quantum phase transition of f-wave FFLO (Fulde-Ferrell-Larkin-Ovchinnikov) superconducting state of spinless fermions on the honeycomb lattice at half filling (see Fig. 3). For an alternative proposal to realize the Wess-Zumino model in condensed matter systems, see Ref. [10].

3 Emergent gauge theory

Fractionalization is a phenomenon where a microscopic particle in many-body systems decay into multiple modes each of which carry a fractional quantum number of the original particle. In contrast to the more familiar phenomena where a composite particle breaks into its constituent particles at high energies, fractionalization is a low energy collective phenomenon where microscopic particles do not ‘really’ break into partons. Instead, many-body correlations make it possible for parts of microscopic particles to emerge as deconfined excitations in the low energy limit [12]. When fractionalization occurs, a gauge field emerges as a collective excitation that mediates interaction between fractionalized excitations. There exist many models which exhibit fractionalization [13–19]. In this lecture, we are going to illustrate this phenomenon using a simple model [20].

3.1 Model

Consider a 4-dimensional Euclidean hypercubic lattice (with discretized time). At each site on the lattice, there are boson fields $e^{i\theta^{ab}}$ which carry one flavor index a and one anti-flavor index b with $a, b = 1, 2, \dots, N$. We impose constraints $\theta^{ab} = -\theta^{ba}$; $e^{i\theta^{ab}}$ is anti-particle of $e^{i\theta^{ba}}$. There are $N(N - 1)/2$ independent boson fields per site. In the following, we will refer to these bosons as ‘mesons’. The action is

$$S = -t \sum_{\langle i,j \rangle} \sum_{a,b} \cos(\theta_i^{ab} - \theta_j^{ab}) - K \sum_i \sum_{a,b,c} \cos(\theta_i^{ab} + \theta_i^{bc} + \theta_i^{ca}). \quad (3.1)$$

Here the first term is the standard Euclidean kinetic energy of bosons and the second term is a flavor conserving interactions between bosons. This model can be viewed as a low energy effective theory of excitons in a multi-band insulator.⁵ But let’s forget about the ‘true UV theory’ and take this model as our microscopic model and regard these bosons as fundamental particles.

3.2 Slave-particle theory

We are interested in the strong coupling limit ($K \gg 1$). In this limit, the large potential energy imposes the dynamical constraints

$$\theta_i^{ab} + \theta_i^{bc} + \theta_i^{ca} = 0 \quad (3.2)$$

for every set of a, b, c . The constraints are satisfied on a $(N - 1)$ -dimensional manifold in $(S^1)^{N(N-1)/2}$ on each site. The low energy manifold is parametrized by

$$\theta_i^{ab} = \phi_i^a - \phi_i^b, \quad (3.3)$$

⁵In this context, an exciton with flavor a and anti-flavor b describes a composite particle made of an electron in the a -th band and a hole in the b -th band of a multi-band insulator.

where the new bosonic fields ϕ^a carry only one flavor quantum number contrary to the meson fields. The new bosons are called slave-particles or partons. They are ‘enslaved’ to each other because these partons can not escape out of mesons. Note that there is a local $U(1)$ redundancy in this parametrization and the low energy manifold is $(S^1)^N/S^1$.

Within this low energy manifold, the potential energy can be dropped and the kinetic energy becomes

$$S = -t \sum_{\langle i,j \rangle} \left[\sum_a e^{i(\phi_i^a - \phi_j^a)} \right] \left[\sum_b e^{-i(\phi_i^b - \phi_j^b)} \right]. \quad (3.4)$$

Since the kinetic energy is factorized in the flavor space, one can introduce a collective dynamical field $\eta \sim \sum_b e^{-i(\phi_i^b - \phi_j^b)}$ using the Hubbard-Stratonovich transformation. Then the effective action becomes

$$S = t \sum_{\langle i,j \rangle} \left[|\eta_{ij}|^2 - |\eta_{ij}| \sum_a e^{i(\phi_i^a - \phi_j^a - a_{ij})} - c.c. \right], \quad (3.5)$$

where a_{ij} is the phase of the complex field η_{ij} . Note that the full theory is invariant under the $U(1)$ gauge transformation

$$\begin{aligned} \phi_i^a &\rightarrow \phi_i^a + \varphi_i, \\ a_{ij} &\rightarrow a_{ij} + \varphi_i - \varphi_j. \end{aligned} \quad (3.6)$$

This theory is a compact $U(1)$ lattice gauge theory coupled with N partons. The bare gauge coupling is infinite because the gauge field does not have a bare kinetic energy term.

One may think that partons are always confined in this theory because the bare gauge coupling is infinite. However, we have to be more careful about what we mean by confinement. Since mesons themselves are fundamental particles, it is indeed impossible to literally separate one meson into two partons. In this sense, a parton is always paired with an anti-parton. However, this confinement at short distance scale does not rule out the possibility that excitations which carry the same quantum number as partons arise as low energy excitations. If such low energy excitations exist, we can say that partons are deconfined in the long distance limit.

How can we understand that partons are deconfined at low energies? To see this, let us integrate out high energy fluctuations of ϕ^a to obtain an effective theory with a cut-off $\Lambda \ll 1/a$ where a is the lattice spacing. The fluctuations of partons generate the Maxwell’s term (and all higher order gauge invariant terms) in the low energy effective action,

$$S = \int dx^4 \left[|(\partial_\mu - ia_\mu)\Phi_a|^2 + V(\Phi_a) + \frac{1}{g^2} F_{\mu\nu} F^{\mu\nu} + \dots \right], \quad (3.7)$$

where $\Phi_a = e^{i\phi^a}$. Due to screening by N charged partons, the gauge coupling is renormalized from infinity down to a finite value $g^2 \sim 1/N$. In the large N limit, the renormalized gauge coupling can be made very small and the deconfinement (Coulomb) phase can arise as a stable phase. Then gapless $U(1)$ gauge boson (emergent photon) and fractionalized bosons (partons) arise as low energy excitations.

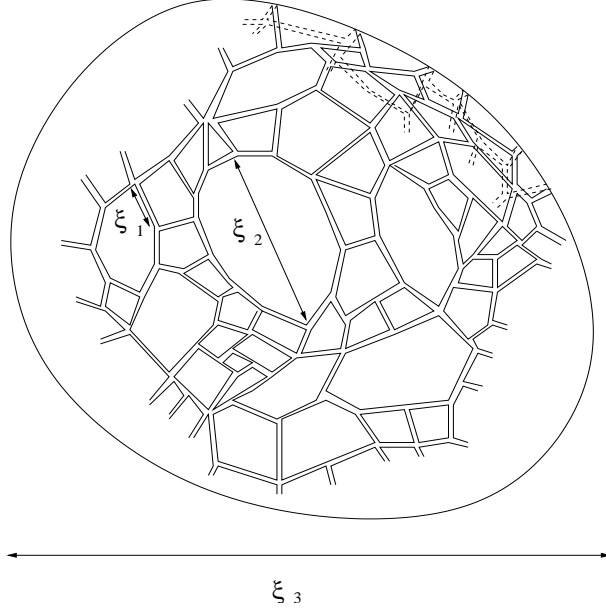


Figure 4: Web of world lines.

3.3 World line picture

Although the above simple argument is plausible, the relation between the ‘slave-partons’ which are confined at short distance scales and the ‘liberated-partons’ which are deconfined at long distance scales is rather obscure in this description. Moreover, it is not entirely clear how partons can screen the gauge field in the first place if they are always confined within neutral mesons. In other words, one can question how one can integrate out high energy fluctuations of partons reliably if they are subject to the infinitely strong gauge coupling at high energies.

For this reason, it is useful to understand fractionalization purely in terms of original mesons without introducing slave particles. Actually one can understand fractionalization intuitively in terms of world lines of mesons. The world line picture is not a quantitative description, but it is useful in that it provides a physical picture for fractionalization. In space-time, world lines of mesons can be represented as double lines with two opposite arrows, where each arrow carries a flavor current.

In the partition function, the simplest configuration is a loop of meson world line made of two overlapped single-line loops with current of flavor a moving in one direction and b in the other direction. General configurations consist of a collection of connected webs made of world lines (world line web). Each world line web defines closed surfaces as depicted in Fig. 4. Many such closed surfaces may co-exist and interpenetrate each other. There are three different length scales in the world line web. The shortest scale is the length of double line segment (ξ_1) which corresponds to the life time of a single meson. As the interaction becomes stronger, mesons decay faster and ξ_1 becomes shorter. The next scale is the typical size of single line loops (ξ_2). This can be much larger than ξ_1 even in the strong coupling limit. This is because a single flavor a can switch as many partners as it wants during its life

time before it meets with its own anti-flavor \bar{a} and decays into vacuum.⁶ In this case, we can view single lines as world lines of emergent long-living excitations. The largest length scale is the size of the bubble made of the web (ξ_3). By tuning three dimensionless parameters in the theory (K , N and t), it is possible to tune three scales, ξ_1/a , ξ_2/a , ξ_3/a , where a is the lattice spacing. Here we will focus on the limit $K \gg 1$ where $\xi_1 \sim a$.⁷

In the small t and small N limit (which corresponds to the limit of very massive mesons), all length scales are of order of the lattice scale. As t increases, mesons become lighter, and ξ_2 increases. As N increases, configurations with many single line loops become more important due to entropic contribution of flavors associated with each single line loops. As a result, the tension of world line web decreases and ξ_3 increases. If $a \sim \xi_1 \ll \xi_2 \ll \xi_3$ (which can be achieved for a large N with fixed tN) the closed surface of the world line web is well-defined in the length scale $\xi_2 \ll x \ll \xi_3$. Thus the effective degrees of freedom at this scale are fluctuating membrane in space-time. The surface can be regarded as the world sheet of oriented closed string.⁸ In the gauge theory picture the string corresponds to electric flux line and the string tension, the gauge coupling. The gauge group should be $U(1)$ due to the orientedness of surfaces, and the effective theory becomes a pure $U(1)$ gauge theory. In this scale, the world line web is very floppy and one obtains a weakly coupled pure gauge theory. The transverse fluctuations of world line web corresponds to emergent gauge bosons.

For a finite ξ_3 , one eventually enters into the region where $x \gg \xi_3$ as one probes longer distance scale. In this long distance limit, there are only small membranes and the vacuum is essentially empty. This corresponds to the confinement phase and ξ_3 corresponds the confining scale.

In the opposite limit, if we lower our length scale x to the scale comparable to ξ_2 , one begins to notice holes on closed surfaces. One can interpret boundaries of the holes as world lines of particles. These particles should be viewed as bosons because each contribution adds up in the partition function without minus signs associated with single line loops. This is related to the fact that e^{-S} and the measure in the partition function are positive definite in the world line basis due to the absence of frustration in this model. The emergent bosons carry unit charge with respect to the gauge field. This is because world line web which corresponds to world sheet of one unit of electric flux line can end on boundaries. Moreover, these bosons carry only one flavor quantum number due to the fact that an anti-flavor b which always accompanies a flavor a is canceled by the flavor b of nearby mesons.⁹ This is analogous to the situation where one can find a nonzero charge density on a surface of a dielectric medium made of charge neutral molecules. Therefore in the scale $x \sim \xi_2$, the effective degrees of freedom are gauge bosons coupled with N fractionalized bosons which carry only one flavor quantum number.

In the shortest length scale $x \ll \xi_2$, loops of single lines look very large and these fractionalized bosons appear to be condensed. It corresponds to the Higgs phase of the gauge theory.

⁶One's life time can be in principle much longer than the average lifetime of marriages.

⁷This condition is not crucial in what follows. In general, one can tune K so that $\xi_1 \gg a$.

⁸The world line web is oriented because single lines are oriented.

⁹Imagine that there is a string of mesons, $ab - bc - cd - de - \dots$. If you look at this string in the scale larger than the average spacing between mesons, you will see only flavor a at the end of the string.

Therefore, for finite ξ_2 and ξ_3 there are crossovers from the behavior of Higgs phase to Coulomb phase and eventually to the confinement as one probes the system at progressively longer distance scales. The crossover within the confinement phase become a real phase transition to a deconfinement phase as ξ_3 is made to diverge by making N larger with fixed tN . If ξ_3 diverges while ξ_2 remains finite, the fractionalized bosons remain gapped but the gauge boson becomes gapless. This is the Coulomb phase.¹⁰

Although a parton is always bound with an anti-parton, it can propagate in space rather freely by switching its partners repeatedly in the Coulomb phase. As a result, partons can be effectively liberated and arise as well-defined excitations in the Coulomb phase.

One may ask why one gets a weakly coupled gauge theory rather than some string theory. One possible answer is that world line web is very dense in space-time in this case. They constantly join and split, and their contact interactions are also important. It is hard to imagine to have a well defined string in this strongly coupled soup of strings. This can be viewed as a Lagrangian (or space-time) picture for the string-net condensation [23].

One can study different types of flavor preserving interactions. In particular, one can obtain fractionalized fermions [20, 23] if one introduces a quartic interaction for mesons,

$$K_4 \sum_{a,b,c,d} \cos(\theta^{ab} + \theta^{bc} + \theta^{cd} + \theta^{da}) \quad (3.8)$$

instead of the cubic interaction. If $K_4 > 0$, the interaction is frustrated and not all terms in the potential energy can be minimized simultaneously. This frustration results in a larger low energy manifold and wavefunctions within the low energy manifold acquires non-trivial sign structure, namely wavefunctions describing low energy excitations are no longer positive definite. This non-trivial sign structure is responsible for the fermionic statistics of emergent excitations. The emergent fermion can be also understood from the world line picture where single line loops are endowed with minus signs in the partition function due to the frustrated interaction. Then one should interpret single line loops as world lines of fermions.

4 Critical spin liquid with Fermi surface

4.1 From spin model to gauge theory

4.1.1 Slave-particle approach to spin-liquid states

Let us consider a system where spins are antiferromagnetically coupled in a two-dimensional lattice,

$$H = J \sum_{\langle i,j \rangle} \vec{S}_i \cdot \vec{S}_j + \dots \quad (4.1)$$

Here we focus on models with spin 1/2. The antiferromagnetic coupling $J > 0$ favors neighboring spins that align in anti-parallel directions. The dots denote higher order spin

¹⁰In 2+1D, Coulomb phase can not be stable with massive partons due to non-perturbative effects [21]. This opens up the possibility that ξ_2 and ξ_3 diverge simultaneously without an additional fine tuning at a critical point [22].

interactions whose specific forms are not important for the following discussion. The spin model can be viewed as a low energy effective theory of the Hubbard model at half-filled insulating phase where charges can not conduct due to a large Coulomb repulsion.

At sufficiently low temperatures $T < J$, spins usually order, spontaneously breaking the SU(2) spin rotational symmetry.¹¹ However, magnetic ordering can be avoided even at zero temperature if quantum fluctuations are strong enough. Two important sources for strong quantum fluctuations are proximity to metallic state and geometrical frustration. In systems which have small charge gap, the ... terms induced by charge fluctuations cause quantum fluctuations of spins (such as permutations of spins around plaquettes) which tend to disrupt magnetic ordering. Quantum fluctuations are also enhanced by geometrical frustrations. Geometrical frustrations arise when no spin configuration can minimize all interaction terms simultaneously in the classical Hamiltonian. For example, antiferromagnetic couplings on the triangular lattice can not be simultaneously minimized. Although there is no magnetic long-range order in disordered ground states, spins remain highly correlated and we refer to such correlated non-magnetic state as spin liquid [24] as opposed to spin gas. More importantly, many-body wavefunctions of spin liquids exhibit non-local entanglement [25] which can be captured only through a new quantum mechanical notion of order [26] which is beyond the scheme of conventional order parameter.

One way of understanding spin liquid states is to use slave-particle approach. For example, one decomposes a spin operator into fermion bilinear

$$\vec{S}_i = \sum_{\alpha\beta} f_{i\alpha}^\dagger \vec{\sigma}_{\alpha\beta} f_{i\beta}. \quad (4.2)$$

Here $f_{i\alpha}$ is a fermionic field which does not carry electromagnetic charge but carry only spin 1/2. For this reason, this particle is called ‘spinon’ This decomposition has the U(1) phase redundancy. As a result, the theory for spinon has to be in the form of gauge theory. A compact U(1) gauge theory coupled with spinons can be derived following a similar step described in the previous lecture. Although the bare gauge coupling is infinite, the coupling is renormalized to a finite value in the low energy limit. If deconfinement phase is stabilized, spinons and the gauge field arise as low energy degrees of freedom.

Since there is spin 1/2 per each site, there is one spinon per site. Although there is no bare kinetic term for spinons, they can propagate in space through the exchange interaction : simultaneous flips of neighboring spins can be viewed as two spinons exchanging their positions. As a result, spinons form a band, which then determines the low energy spectrum. In non-bipartite lattice (a lattice which can not be divided into A and B sublattices, such as the triangular lattice), the fermions generically form a Fermi surface at half filling. In this case, the low energy effective theory has a Fermi surface of spinons coupled with the emergent U(1) gauge field [27, 28],

$$S = \int d^3x \left[\Psi_j^* (\partial_0 - ia_0 - \mu_F) \Psi_j + \frac{1}{2m} \Psi_j^* (-i\nabla - \mathbf{a})^2 \Psi_j + \frac{1}{4g^2} f_{\mu\nu} f_{\mu\nu} \right]. \quad (4.3)$$

¹¹We can treat the SU(2) symmetry as an internal symmetry in the absence of the spin-orbit coupling which is typically small.

Here Ψ_j is the fermion field with two flavors, $j = 1, 2$ (spin up and down) and $a_\mu = (a_0, \mathbf{a})$ is the U(1) gauge field with $\mu = 0, 1, 2$. μ_F is the chemical potential and g , the gauge coupling. This is nothing but the three dimensional quantum electrodynamics (QED3) with a nonzero chemical potential.

The zeroth order question one has to ask is the stability of the deconfinement phase. Because of the presence of underlying lattice, the U(1) gauge field is compact. This allows for instanton (or monopole) which describes an event localized in time where the flux of the gauge field changes by 2π . It is known that if there is no gapless spinon, instantons always proliferate in space-time, resulting in confinement [21].¹² In this case, spin liquid states are not stable and spinons are confined. In the presence of gapless spinons, it is possible that the gauge field is screened and instanton becomes irrelevant in the low energy limit [32]. If this happens, fractionalized phase is stable and spinons arise as low energy excitations.

If there are a large number of gapless spinons which have the relativistic dispersion, instanton acquires a scaling dimension proportional to the number of flavors N [33–36] and the fractionalized phase is stable. In the presence of spinon Fermi surface, it turns out that the deconfinement phase can be stable for any nonzero fermion flavor.

4.1.2 Stability of deconfinement phase in the presence of Fermi surface

To show that instanton is irrelevant in the presence of Fermi surface, we need the following four ingredients [37].

First, one can describe low energy particle-hole excitations near the Fermi surface in terms of an infinite copy of 1+1 dimensional fermions parametrized by the angle around the Fermi surface [38]. In this angular representation, instanton becomes a twist operator which twists the boundary condition of the 1+1D fermions by π . In the presence of an instanton, the fermions become anti-periodic around the origin in the 1+1D space-time. This can be understood in the following way. At each point on the Fermi surface, the Fermi velocity is perpendicular to the Fermi surface. A fermion (or a wave packet made of states near a point on the Fermi surface) with a given Fermi velocity explores a 1+1 dimensional subspace in real space which is perpendicular to the x-y plane in 2+1D. Since instanton is a source of 2π flux localized in space-time, the total flux of π penetrates through this plane. (Here we are assuming that there is the rotational symmetry. But this argument can be generalized to cases without the symmetry.) Therefore, a fermion moving in the plane encloses a flux close to π as it is transported around the origin at a large distance. As a result, the boundary condition of low energy fermion at each angle is twisted by π .

Second, the angle θ around the Fermi surface has a positive scaling dimension. As a result, the angle is decompactified and runs from $-\infty$ to ∞ in the low energy limit. In the low energy limit, the gauge field becomes more and more ineffective in scattering fermions from one momentum to another momentum along tangential directions to the Fermi surface. This is because the momentum of the gauge field becomes much smaller than the Fermi momentum. This amounts to saying that effective angular separation between two fixed points on the Fermi surface grows in the low energy limit.

¹²An exception is when the time-reversal symmetry is broken. In this case, the Chern-Simons term suppresses instanton, stabilizing chiral spin liquid state [29]. Another route of stabilizing deconfinement phase is to break the U(1) gauge group into a discrete gauge group, such as Z_2 [30, 31].

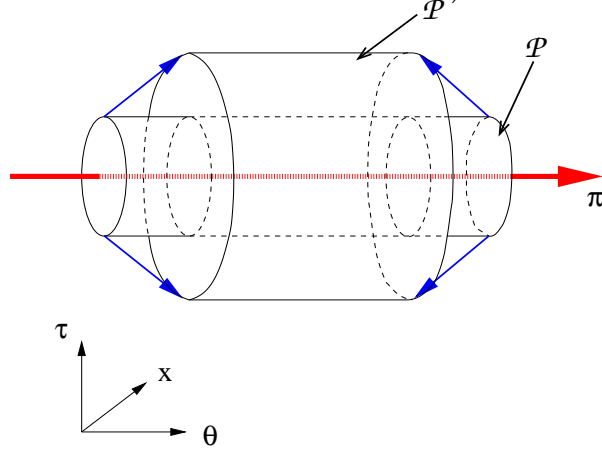


Figure 5: ‘Time’-evolution of a quantum state defined on the surface of a pipe extended along the angular direction, where a π -vortex is pierced through the pipe. Under the time-evolution, a point on the surface \mathcal{P} is mapped to a point on the surface \mathcal{P}' .

Third, the theory is local in the space of the decompactified angle. This is due to the curvature of the Fermi surface. In the low energy limit, only those fermions very close to the Fermi surface can be excited. Since gauge boson scatters one fermion near the Fermi surface to another point near the Fermi surface, the momentum of gauge boson is almost tangential to the Fermi surface where the fermions are located. Therefore, fermions with a particular angle are coupled only with those gauge field whose momentum is tangential to the Fermi surface at the angle in the low energy limit. This means that fermions with a finite angular separation (except for those which are at the exact opposite sides of the Fermi surface) becomes essentially decoupled in the low energy limit because they are coupled only with those gauge bosons whose momenta are separated in the momentum space.

Finally, instanton become a π vortex which is extended along the non-compact θ direction in the theory written in the space of θ , τ and x , where x is a real space coordinate associated with the radial momentum at each point on the Fermi surface. In analogy with the state-operator correspondence in relativistic CFT, the vortex defines a quantum state on the surface of a pipe \mathcal{P} which is extended in the θ direction in the space of τ , x and θ as is shown in Fig. 5. The scaling dimension of instanton corresponds to the ‘energy’ of this quantum state associated with the radial time evolution.

Because of the locality along the decompactified angular direction, the extended π -vortex should have an infinite ‘energy’. This implies that the scaling dimension of instanton diverges and instanton remains strongly irrelevant. As a result, the deconfinement phase is stable.

4.2 Low energy effective theory

Having established that deconfinement phase is stable, we can treat the theory as a non-compact U(1) gauge theory. In this lecture, we are going to analyze the low energy effective theory of Fermi surface coupled with the U(1) gauge field in 2+1D [40–49]. Although we motivated this theory in the context of spin liquid, the same theory often arises in other systems. More importantly, the theory represents a class of typical non-Fermi liquid states which arise

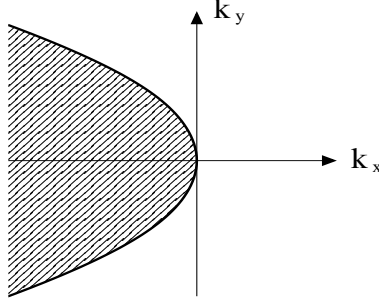


Figure 6: The parabolic Fermi surface of the model in Eq. (4.4). The shaded region includes negative energy states.

as a result of coupling between Fermi surface and gapless bosons. Not surprisingly, many features of this theory are shared by other non-Fermi liquid states in 2+1D [50–58].

In this system, there is no tunable parameter other than the number of fermion (vector) flavors N . Given that the physically relevant theory ($N = 2$) is a strongly coupled theory, it is natural to consider the theory with a large number of fermion flavors N . Naively one would expect that the theory becomes classical in the large N limit. However, this intuition based on relativistic field theories is incorrect in the presence of Fermi surface. Unlike those theories where gapless excitations are located only at discrete set of points in the momentum space, Fermi surface has an extended manifold of gapless points. The abundant low energy excitations subject to the strong IR quantum fluctuations in 2+1D make the theory quite nontrivial even in the large N limit [48].

In the low energy limit, fermions whose velocities are not parallel or anti-parallel to each other are essentially decoupled. As a result, it is sufficient to consider local patches of Fermi surface in the momentum space. The minimal model in parity symmetric systems is the theory which includes an open patch of Fermi surface and one more patch whose Fermi velocity is opposite to that of the former.

Here, we will focus on one patch in the momentum space. The one-patch theory is already quite non-trivial and the full structure is yet to be understood. The two-patch theory has yet another level of complications [49] over which we have much less theoretical control. The action in the one-patch theory is

$$\begin{aligned}
\mathcal{L} = & \sum_j \psi_j^* (\partial_\tau - iv_x \partial_x - v_y \partial_y^2) \psi_j \\
& + \frac{e}{\sqrt{N}} \sum_j a \psi_j^* \psi_j \\
& + a [-\partial_\tau^2 - \partial_x^2 - \partial_y^2] a,
\end{aligned} \tag{4.4}$$

where ψ_j represent fermions with flavor $j = 1, 2, \dots, N$. We have chosen our $\mathbf{k} = 0$ to be the point on the Fermi surface where the Fermi velocity is parallel to the x -direction. v_x is the Fermi velocity and $v_y \sim \frac{1}{m}$ determines the curvature of the Fermi surface. The Fermi surface is on $v_x k_x + v_y k_y^2 = 0$ as is shown in Fig. 6. This is a ‘chiral Fermi surface’ where the x -component of Fermi velocity is always positive. This chirality is what makes the one-patch theory more tractable compared to the two-patch theory. a is the transverse component of

an emergent U(1) gauge boson in the Coulomb gauge $\nabla \cdot \mathbf{a} = 0$. We ignore the temporal component of the gauge field which becomes massive due to screening. The transverse gauge field remains gapless. e is the coupling between fermions and the critical boson.

Quantum fluctuations of gapless modes generate singular self energies. The one-loop quantum effective action becomes

$$\begin{aligned} \Gamma &= \sum_j \int dk \left[i \frac{c}{N} \operatorname{sgn}(k_0) |k_0|^{2/3} + ik_0 + v_x k_x + v_y k_y^2 \right] \psi_j^*(k) \psi_j(k) \\ &+ \int dk \left[\gamma \frac{|k_0|}{|k_y|} + k_0^2 + k_x^2 + k_y^2 \right] a^*(k) a(k) \\ &+ \frac{e}{\sqrt{N}} \sum_j \int dk dq a(q) \psi_j^*(k+q) \psi_j(k), \end{aligned} \quad (4.5)$$

where c and γ are constants of the order of 1. In the low energy limit, the leading terms of the quantum effective action are invariant under the scale transformation,

$$\begin{aligned} k_0 &= b^{-1} k'_0, \\ k_x &= b^{-2/3} k'_x, \\ k_y &= b^{-1/3} k'_y, \\ \psi_a(b^{-1} k'_0, b^{-2/3} k'_x, b^{-1/3} k'_y) &= b^{4/3} \psi'_a(k'_0, k'_x, k'_y). \end{aligned} \quad (4.6)$$

Dropping terms that are irrelevant under this scaling, we write the minimal action as

$$\begin{aligned} \mathcal{L} &= \sum_j \psi_j^* (\eta \partial_\tau - iv_x \partial_x - v_y \partial_y^2) \psi_j \\ &+ \frac{e}{\sqrt{N}} \sum_j a \psi_j^* \psi_j + a (-\partial_y^2) a. \end{aligned} \quad (4.7)$$

Note that the local time derivative term in the fermion action is also irrelevant, and η flows to zero in the low energy limit. But we can not drop this term from the beginning. Otherwise, the theory becomes completely local in time and there is no propagating mode. The role of this irrelevant η -term is to generate a non-trivial frequency dependent dynamics by maintaining the minimal causal structure of the theory before it dies off in the low energy limit. In other words, the η -term itself is irrelevant but it is crucial to generate singular self energies. But once we include the frequency dependent self energies, we can drop the η -term as far as we remember that the non-local self energies have been dynamically generated from the local Lagrangian.

The minimal action (4.7) has four marginal terms. On the other hand, there are five parameters that set the scales of energy-momentum and the fields. Out of the five parameters, only four of them can modify the coefficients of the marginal terms because the marginal terms remain invariant under the transformation (4.6). Using the remaining four parameters, one can always rescale the coefficients of the marginal terms to arbitrary values. Therefore, there is no dimensionless parameter in this theory except for the fermion flavor N . In particular, the gauge coupling e can be always scaled away. This implies that the theory with fixed N flows to a unique fixed point rather than a line of fixed point which has exact marginal deformation. In the following, we will set $v_x = v_y = e = 1$.

4.2.1 Failure of a perturbative $1/N$ expansion

In the naive N counting, a vertex contributes $N^{-1/2}$ and a fermion loop contributes N^1 . In this counting, only the fermion RPA diagram is of the order of 1, and all other diagrams are of higher order in $1/N$. In the leading order, the propagators become

$$\begin{aligned} g_0(k) &= \frac{1}{i\eta k_0 + k_x + k_y^2}, \\ D(k) &= \frac{1}{\gamma \frac{|k_0|}{|k_y|} + k_y^2}. \end{aligned} \quad (4.8)$$

One can attempt to compute the full quantum effective action by including $1/N$ corrections perturbatively. However, it turns out vertex functions which connect fermions on the Fermi surface generically have strong IR singularity, which is cured only by loop corrections. Therefore it is crucial to include the fermion self energy in the dressed fermion propagator,

$$g(k) = \frac{1}{i\eta k_0 + i\frac{c}{N} \text{sgn}(k_0)|k_0|^{2/3} + k_x + k_y^2}. \quad (4.9)$$

Although the self energy has an additional factor of $1/N$ compared to the bare frequency dependent term, the self energy dominates at sufficiently low energy $k_0 < 1/(\eta N)^3$ for any fixed N . Here it is important to take the low energy limit first before taking large N limit. This is the correct order of limits to probe low energy physics in any physically relevant systems with finite N .

The removal of IR singularity does not come without price. In the presence of the self energy, the IR singularity is cut-off at a scale proportional to $1/N$. As a result the IR singularity is traded with a finite piece which has an additional positive power of N . For

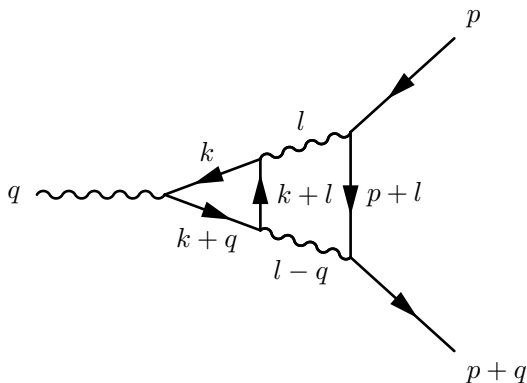


Figure 7: A two-loop vertex correction.

example, the two-loop vertex function (Fig. 7) computed using the bare propagator becomes

$$\Gamma^{bare}(p=0, q) = -\frac{N^{-3/2}}{\eta q_0^{1/3}} f_1(q_y/q_0^{1/3}) \quad (4.10)$$

when both $p=0$ and $p+q$ are on the Fermi surface. Here $f_1(t)$ is a non-singular universal function which is independent of N and η . Note that the vertex function diverges as q goes

to zero with fixed $q_y/q_0^{1/3}$. With the dressed propagator, the IR singularity disappears but there exists an enhancement factor of N ,

$$\Gamma^{dressed}(0, q) = -N^{-1/2} f_2(q_y/q_0^{1/3}), \quad (4.11)$$

where $f_2(t)$ is a non-singular universal function independent of N . Note that this two-loop vertex correction has the same order as the bare vertex, which signals a breakdown of perturbative $1/N$ expansion. Similar enhancement factors arise in other diagrams as well.

4.2.2 Genus Expansion

There exists a simple way of understanding this enhancement factor systematically. The reason why the enhancement factor arises is that the fermion propagator is not always order of 1. For generic momentum away from the Fermi surface, the kinetic energy dominates and the propagator is order of 1. On the other hand, when fermions are right on the Fermi surface, the kinetic energy vanishes and there are only frequency dependent terms. At sufficiently low frequencies, the non-local self energy dominates and the propagator is enhanced to the order of N . In relativistic field theories, there are only discrete set of points in the momentum space where the kinetic energy vanishes. In contrast, there is one dimensional manifold of gapless points in the present case with Fermi surface. Whenever fermions hit the Fermi surface (there are many ways to do that), the fermion propagator gets enhanced to order of N . This is the basic reason why the naive N counting breaks down in the presence of Fermi surface.

For a given diagram, say L -loop diagram, there are $2L$ integrations of internal momenta k_x and k_y .¹³ In the $2L$ -dimensional space of internal momenta, in general there is a m -dimensional sub-manifold on which all internal fermions stay right on the Fermi surface as long as external fermions are on the Fermi surface. We refer to this manifold as ‘singular manifold’. If we focus on the momentum integration near a generic point on the singular manifold, it generically looks like

$$I \sim \int dq_1 dq_2 \dots dq_m \int dk_1 dk_2 \dots dk_{2L-m} \prod_{i=1}^{I_f} \left[\frac{1}{\alpha_j^i k_j + i \frac{1}{N} f(\omega_i)} \right]. \quad (4.12)$$

Here q_1, q_2, \dots, q_m are deviation of momenta from the point on the singular manifold along the directions tangential to the singular manifold. $k_1, k_2, \dots, k_{2L-m}$ are momentum components which are perpendicular to the singular manifold. I_f is the number of fermion propagators. The key point is that the fermion propagators depend only on k 's but not on q 's because kinetic energy of fermions stay zero within the singular manifold. The tangential momenta q 's parametrize exact zero modes of Fermi surface deformations where fermions on the Fermi surface slide along the Fermi surface. If N is strictly infinite and we drop the frequency dependent term in the propagators, the fermion propagators become singular whenever fermions are on the Fermi surface. The m integrations along the tangential direction of the singular manifold do not help to remove the IR singularity. Only $2L - m$ integrations of k momenta lower the degree of IR singularity. After the integration over the

¹³The frequency integrals do not play an important role as far as N counting is concerned.

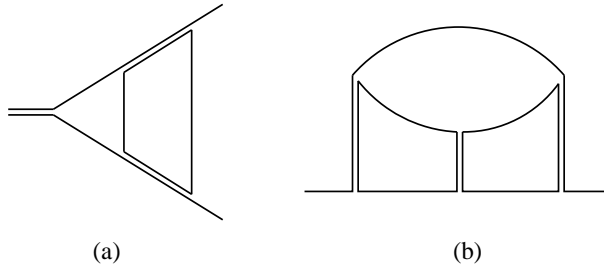


Figure 8: The double line representations of (a) the 2-loop vertex correction and (b) the 3-loop fermion self energy. Double lines represent propagators of the boson, and the single lines are the propagators of the fermion. The number of single line loops (one in (a) and two in (b)) represents the dimension of the singular manifold (see the text) on which all fermions remain on the Fermi surface in the space of internal momenta.

all $2L$ momentum, the remaining IR singularity is order of $I_f - (2L - m)$. For a finite N , this IR singularity is cut-off at a momentum proportional to $1/N$. This means the resulting diagram has an additional factor of $N^{I_f - (2L - m)}$ as compared to the naive N counting.

What determines the dimension of the singular manifold within which fermions always remain on the Fermi surface? It turns out that the dimension of the singular manifold is given by the number of closed loops when one draws boson propagators using double lines and fermion propagators using single lines [38,39]. First, we restrict momenta of all fermions to be on the Fermi surface. A momentum \mathbf{k}_θ of fermion on the Fermi surface is represented by an one-dimensional parameter θ . Then, a momentum of the boson \mathbf{q} is decomposed into two momenta on the Fermi surface as $\mathbf{q} = \mathbf{k}_\theta - \mathbf{k}_{\theta'}$, where both \mathbf{k}_θ and $\mathbf{k}_{\theta'}$ are on the Fermi surface. This decomposition is unique because there is only one way of choosing such \mathbf{k}_θ and $\mathbf{k}_{\theta'}$. As far as momentum conservation is concerned, one can view the boson of momentum \mathbf{q} as a composite particle made of a fermion of momentum \mathbf{k}_θ and a hole of momentum $\mathbf{k}_{\theta'}$. For example, the two-loop vertex correction and the three-loop fermion self energy correction can be drawn as Fig. 8 in this double line representation. In this representation, each single line represents a momentum on the Fermi surface. Momenta in the single lines that are connected to the external lines should be uniquely fixed in order for all fermions to stay on the Fermi surface. On the other hand, momenta on the single lines that form closed loops by themselves are unfixed. In other words, all fermions can stay on the Fermi surface no matter what the value of the unfixed momentum component that runs through the closed loop is. Since there is one closed loop in Fig. 8 (a), the dimension of the singular manifold is 1 and the enhancement factor becomes $N^{4 - (4 - 1)} = N$ for the two-loop vertex correction. Likewise, the enhancement factor for the three-loop fermion self energy becomes $N^{5 - (6 - 2)} = N$ which makes the three-loop fermion self energy to have the same power $1/N$ as the one-loop correction.

The enhancement factor is a direct consequence of the presence of infinitely many soft modes associated with deformations of Fermi surface. The extended Fermi surface makes it possible for virtual particle-hole excitations to maneuver on the Fermi surface without costing much energy. As a result, quantum fluctuations becomes strong when external momenta are arranged in such a way that there are sufficiently many channels for the virtual particle-

hole excitations to remain on the Fermi surface. This makes higher order processes to be important even in the large N limit. We note that this effect is absent in relativistic quantum field theories where gapless modes exist only at discrete points in the momentum space.

The net power in N for general Feynman diagrams becomes

$$N^{-V/2+L_f+[n+\frac{E_f+2E_b}{2}-2]}, \quad (4.13)$$

where n is the number of single line loop, E_f (E_b) is the number of external lines for fermion (boson), and L_f is the number of fermion loop. Here $[x] = x$ for non-negative x and $[x] = 0$ for negative x . For vacuum diagram, the N -counting depends only on the topology of the Feynman diagram and it becomes

$$N^{-2g}, \quad (4.14)$$

where g is the genus of the 2d surface on which Feynman graph is drawn using the full double line representation without any crossing. In the full double line representation, we draw not only the boson propagator as a double line, but also the fermion propagator as a double line where the additional line associated with a fermion loop corresponds to the flavor degree of freedom which run from 1 to N . As a result, all planar diagrams are generically order of N^0 . Some typical planar diagrams are shown in Figs. 9 and 10.

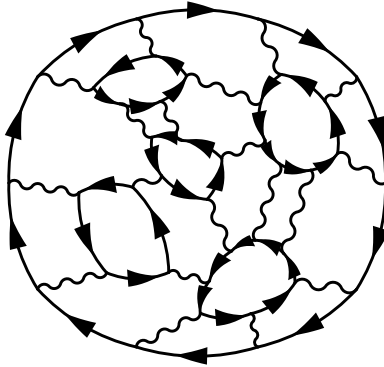


Figure 9: A typical vacuum planar diagram which is of the order of N^0 .

The above counting is based on the local consideration on the space of internal momenta near the singular manifold. It turns out that planar diagrams precisely follow the counting obtained from this local considerations. Some non-planar diagrams may deviate from this local counting by some factor of $\log N$. The full structure of non-planar diagrams are not completely understood yet.

Power counting of diagrams with external lines can be easily obtained from the counting of vacuum diagrams. The leading contributions come from the planar diagrams where the genus of the underlying 2d surface is zero. In principle, there can be infinitely many diagrams which are order of N^0 (N^{-1}) for the boson (fermion) self energy and $N^{-1/2}$ for the three-point vertex function.

Because the one-patch theory is a chiral theory, there are strong kinematic constraints. Using this, one can prove that all planar diagrams for boson self energy vanish beyond the one loop. Moreover one can show that the beta function vanishes and fermions have no anomalous

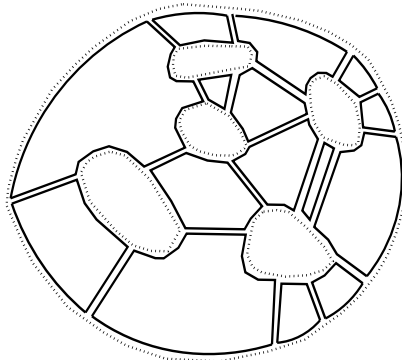


Figure 10: The full double line representation of the planar diagram shown in Fig. 9. The solid double lines represent the boson propagator and double lines made of one solid and one dotted lines represent fermion propagators. Loops of dotted lines are added to each fermion loops. In this representation, there is a factor of N for each closed single line loop whether it is a loop made of a solid or dotted line.

scaling dimension to the leading order of N (the contributions of planar diagrams). However, there are still infinitely many non-vanishing planar diagrams for the fermion self energy and the vertex function.

Although the present theory has fermions with vector flavors, it behaves like a matrix model in the large N limit. The reason why the genus expansion arises from this vector model is that the angle around the Fermi surface plays the role of an additional flavor. In the usual matrix model, N controls the genus expansion and the 't Hooft coupling λ controls the loop expansion. One expects that a continuum world sheet description of string emerges in a matrix model when both N and λ are large. In the present case, the effective 't Hooft coupling is order of 1. In other words, two diagrams with L -loops and $(L + 1)$ -loops have the same order of magnitude as far as they have same topology. This is because there is no dimensionless parameter in the theory other than N as discussed earlier. With $\lambda \sim 1$, it is unlikely that one can use a dual gravity description in a weakly curved space-time to understand this non-Fermi liquid state. Recently, it has been pointed out that the non-Fermi liquid states studied from classical gravity [60–69] show phenomenology of a system where Fermi surface is coupled with a large number of localized bosonic degrees of freedom [70].

One may view the present theory as a weakly coupled string theory in a highly curved background. It would be interesting to find a way to stabilize the theory at a large 't Hooft coupling. However, this appears to be difficult to achieve in non-supersymmetric theories due to instabilities.

If one includes two patches of Fermi surface, even non-planar diagrams are important due to UV divergence, and the genus expansion appears to break down [49]. It is yet to be understood how Feynman diagrams are organized in this case. On the other hand, one can perturbatively control the theory if one introduces an additional control parameter besides

1/N [59].

5 Holographic description of quantum field theory

Although the AdS/CFT correspondence has been conjectured based on the superstring theory, it is possible that the underlying holographic principle is more general and a wider class of quantum field theories can be understood through holographic descriptions [71–75]. According to the holographic principle, the partition function of a D-dimensional theory can be written as a partition function of a (D+1)-dimensional theory where the information on the D-dimensional theory is encoded through boundary conditions as

$$\begin{aligned} Z[J(x)] &= \int D\phi(x) e^{-S^D[\phi] - \int dx J\phi} \\ &= \int D “J(x, z)” e^{-S^{(D+1)}[J(x, z)]} \Big|_{J(x, 0)=J(x)}, \end{aligned} \tag{5.1}$$

where $J(x, z)$ represent (D+1)-dimensional degrees of freedom. It is most likely that the holographic description will be useful only for quantum field theories which satisfy certain conditions, such as factorization of correlation functions and a large gap in the spectrum of scaling dimensions. Nevertheless, it would be still useful to develop a general prescription for the mapping. In this lecture, we will present a prescription that may be useful in deriving holographic theory for general quantum field theory [75].

5.1 Toy-model : 0-dimensional scalar theory

To illustrate the basic idea, we first consider the simplest field theory : 0-dimensional scalar theory. In zero dimension, the partition function is given by an ordinary integration,

$$Z[\mathcal{J}] = \int d\Phi e^{-S[\Phi]}. \tag{5.2}$$

We consider an action $S[\Phi] = S_M[\Phi] + S_{\mathcal{J}}[\Phi]$ with

$$\begin{aligned} S_M[\Phi] &= M^2\Phi^2, \\ S_{\mathcal{J}}[\Phi] &= \sum_{n=1}^{\infty} \mathcal{J}_n \Phi^n. \end{aligned} \tag{5.3}$$

Here S_M is the bare action with ‘mass’ M . $S_{\mathcal{J}}$ is a deformation with sources \mathcal{J}_n . For simplicity, we will consider deformations upto quartic order : $\mathcal{J}_n = 0$ for $n > 4$. Here is the prescription to construct a holographic theory.

- Step 1. Introduce an auxiliary field [76].

We add an auxiliary field $\tilde{\Phi}$ with mass μ ,

$$Z[\mathcal{J}] = \mu \int d\Phi d\tilde{\Phi} e^{-(S[\Phi] + \mu^2\tilde{\Phi}^2)}. \tag{5.4}$$

Then, we find a new basis ϕ and $\tilde{\phi}$

$$\begin{aligned}\Phi &= \phi + \tilde{\phi}, \\ \tilde{\Phi} &= A\phi + B\tilde{\phi},\end{aligned}\tag{5.5}$$

in such a way that the ‘low energy field’ ϕ has a mass M' which is slightly larger than the original mass M , and the ‘high energy field’ $\tilde{\phi}$ has a large mass m' ,

$$\begin{aligned}M'^2 &= M^2 e^{2\alpha dz}, \\ m'^2 &= \frac{M^2}{2\alpha dz},\end{aligned}\tag{5.6}$$

where dz is an infinitesimally small parameter and α is a positive constant. Quantum fluctuations for ϕ become slightly smaller than the original field Φ . The missing quantum fluctuations are compensated by the high energy field $\tilde{\phi}$. In terms of the new variables, the partition function is written as

$$Z[\mathcal{J}] = \left(\frac{Mm'}{M'} + \frac{MM'}{m'} \right) \int d\phi d\tilde{\phi} e^{-(S_{\mathcal{J}}[\phi+\tilde{\phi}] + M'^2\phi^2 + m'^2\tilde{\phi}^2)}.\tag{5.7}$$

- Step 2. Rescale the fields.

To maintain the same form for the quadratic action, we rescale the fields as

$$\phi \rightarrow e^{-\alpha dz} \phi, \quad \tilde{\phi} \rightarrow e^{-\alpha dz} \tilde{\phi}.\tag{5.8}$$

Then the couplings are rescaled as $\mathcal{J}_n \rightarrow j_n = \mathcal{J}_n e^{-n\alpha dz}$ and $m \rightarrow m' e^{-\alpha dz}$.

- Step 3. Expand the action in the power series of the low energy field.

The new action becomes

$$\begin{aligned}S_j[\phi + \tilde{\phi}] &= S_j[\tilde{\phi}] + (j_1 + 2j_2\tilde{\phi} + 3j_3\tilde{\phi}^2 + 4j_4\tilde{\phi}^3)\phi \\ &\quad + (j_2 + 3j_3\tilde{\phi} + 6j_4\tilde{\phi}^2)\phi^2 + (j_3 + 4j_4\tilde{\phi})\phi^3 + j_4\phi^4.\end{aligned}\tag{5.9}$$

In the standard renormalization group (RG) procedure [77], one integrates out the high energy field to obtain an effective action for the low energy field with renormalized coupling constants. Here we take an alternative view and interpret the high energy field $\tilde{\phi}$ as fluctuating sources for the low energy field. This means that the sources for the low energy field can be regarded as dynamical fields instead of fixed coupling constants.

- Step 4. Decouple low energy field and high energy field.

We decouple the high energy field and the low energy field by introducing Hubbard-Stratonovich fields J_n and P_n ,

$$Z[\mathcal{J}] = m \int d\phi d\tilde{\phi} \Pi_{n=1}^4 (dJ_n dP_n) e^{-(S'_j + M^2\phi^2 + m^2\tilde{\phi}^2)},\tag{5.10}$$

where

$$\begin{aligned}
S'_j &= S_j[\tilde{\phi}] \\
&+ iP_1 J_1 - iP_1(j_1 + 2j_2\tilde{\phi} + 3j_3\tilde{\phi}^2 + 4j_4\tilde{\phi}^3) + J_1\phi \\
&+ iP_2 J_2 - iP_2(j_2 + 3j_3\tilde{\phi} + 6j_4\tilde{\phi}^2) + J_2\phi^2 \\
&+ iP_3 J_3 - iP_3(j_3 + 4j_4\tilde{\phi}) + J_3\phi^3 \\
&+ iP_4 J_4 - iP_4 j_4 + J_4\phi^4.
\end{aligned} \tag{5.11}$$

- Step 5. Integrate out the high energy mode.

We integrate out $\tilde{\phi}$ to the order of dz . The auxiliary fields P and J acquire non-trivial action,

$$Z[\mathcal{J}] = \int d\phi \Pi_{n=1}^4 (dJ_n dP_n) e^{-(S_J[\phi] + M^2\phi^2 + S^{(1)}[J,P])}, \tag{5.12}$$

where

$$\begin{aligned}
S^{(1)}[J,P] &= \sum_{n=1}^4 i(J_n - \mathcal{J}_n + n\alpha dz \mathcal{J}_n) P_n \\
&+ \frac{\alpha dz}{2M^2} (i\tilde{\mathcal{J}}_1 + 2P_1\tilde{\mathcal{J}}_2 + 3P_2\tilde{\mathcal{J}}_3 + 4P_3\tilde{\mathcal{J}}_4)^2,
\end{aligned} \tag{5.13}$$

and $\tilde{\mathcal{J}}_n = (\mathcal{J}_n + J_n)/2$. One can explicitly check that the above action reproduces all renormalized coupling to the order of dz if P_n and J_n are integrated out.

- Step 6. Repeat the steps 1-5 for the low energy field

If we keep applying the same procedure to the low energy field, the partition function can be written as a functional integration over fluctuating sources and conjugate fields,

$$Z[\mathcal{J}] = \int \Pi_{n=1}^4 (DJ_n DP_n) e^{-S[J,P]}, \tag{5.14}$$

where

$$\begin{aligned}
S[J,P] &= \int_0^\infty dz \left[i(\partial_z J_n + n\alpha J_n) P_n \right. \\
&\left. + \frac{\alpha}{2M^2} (iJ_1 + 2P_1 J_2 + 3P_2 J_3 + 4P_3 J_4)^2 \right].
\end{aligned} \tag{5.15}$$

Here $DJ_n DP_n$ represent functional integrations over one dimensional fields $J_n(z), P_n(z)$ which are defined on the semi-infinite line $[0, \infty)$. The boundary value of $J_n(z)$ is fixed by the coupling constants of the original theory, $J_n(0) = \mathcal{J}_n$. $P_n(z)$ is the conjugate field of $J_n(z)$ which describes physical fluctuations of the operator ϕ^n . This can be seen from the equations of motion for J_n .

The theory given by Eqs. (5.14) and (5.15), which is exactly dual to the original theory, is an one-dimensional local quantum theory. The emergent dimension z corresponds to logarithmic energy scale [78]. The parameter α determines the rate the energy scale is changed. The partition function in Eq. (5.14) does not depend on the rate high energy modes are eliminated as far as all modes are eventually eliminated. Moreover, at each step of mode elimination, one could have chosen α differently. Therefore, α can be regarded as a function of z . If one interprets z as ‘time’, it is natural to identify $\alpha(z)$ as the ‘lapse function’, that is, $\alpha(z) = \sqrt{g_{zz}(z)}$, where $g_{zz}(z)$ is the metric. Then one can view Eqs. (5.14) and (5.15) as an one-dimensional gravitational theory with matter fields J_n . This becomes more clear if we write the Lagrangian as

$$L = P_n \partial_z J_n - \alpha H, \quad (5.16)$$

where H is the Hamiltonian (the reason why H is not Hermitian is that we started from the Euclidean field theory). However, there is one difference from the usual gravitational theory. In the Hamiltonian formalism of gravity [79], the lapse function is a Lagrangian multiplier which imposes the constraint $H = 0$. However, in Eq. (5.14), α is not integrated over and the Hamiltonian constraint is not imposed. This is due to the presence of the boundary at $z = 0$ which explicitly breaks the reparametrization symmetry. In particular, the ‘proper time’ from $z = 0$ to $z = \infty$ given by

$$l = \int_0^\infty \alpha(z) dz \quad (5.17)$$

is a quantity of physical significance which measures the total warping factor. To reproduce the original partition function in Eq. (5.2) from Eq. (5.14), one has to make sure that $l = \infty$ to include all modes in the infrared limit. Therefore, l should be fixed to be infinite. As a result, one should not integrate over all possible $\alpha(z)$ some of which give different l . This is the physical reason why the Hamiltonian constraint is not imposed in the present theory. This theory can be viewed as a gravitational theory with the fixed size along the z direction.

Although there are many fields in the bulk, i.e. J_n, P_n for each n , there is only one propagating mode, and the remaining fields are non-dynamical in the sense they strictly obey constraints imposed by their conjugate fields. This is not surprising because we started with one dynamical field Φ . There is a freedom in choosing one independent field. In this case, it is convenient to choose J_3 as an independent field. If one eliminates all dependent fields, one can obtain the local bulk action for one independent field.

5.2 D -dimensional $O(N)$ vector theory

The same procedure can be generalized to D -dimensional field theory. For example, the partition function for the D -dimensional $O(N)$ vector model,

$$\begin{aligned} S[\Phi] &= \int d\mathbf{x} d\mathbf{y} \Phi_a(\mathbf{x}) G_M^{-1}(\mathbf{x} - \mathbf{y}) \Phi_a(\mathbf{y}) \\ &+ \int d\mathbf{x} \left[\mathcal{J}_a \Phi_a + \mathcal{J}_{ab} \Phi_a \Phi_b + \mathcal{J}_{abc} \Phi_a \Phi_b \Phi_c + \mathcal{J}_{abcd} \Phi_a \Phi_b \Phi_c \Phi_d \right. \\ &\left. + \mathcal{J}_{ab}^{ij} \partial_i \Phi_a \partial_j \Phi_b + \mathcal{J}_{abc}^{ij} \Phi_a \partial_i \Phi_b \partial_j \Phi_c + \mathcal{J}_{abcd}^{ij} \Phi_a \Phi_b \partial_i \Phi_c \partial_j \Phi_d \right] \end{aligned} \quad (5.18)$$

can be written as a $(D + 1)$ -dimensional functional integration,

$$Z[\mathcal{J}] = \int DJDP e^{-S[J,P]}, \quad (5.19)$$

where the bulk action is given by

$$\begin{aligned} S[J, P] = \int d\mathbf{x}dz & \left\{ iP_a(\partial J_a - \frac{2+D}{2}\alpha J_a) + iP_{ab}(\partial J_{ab} - 2\alpha J_{ab}) + iP_{ab,ij}(\partial J_{ab}^{ij}) \right. \\ & + iP_{abc}(\partial J_{abc} - \frac{6-D}{2}\alpha J_{abc}) + iP_{abc,ij}(\partial J_{abc}^{ij} - \frac{2-d}{2}\alpha J_{abc}^{ij}) \\ & \left. + iP_{abcd}(\partial J_{abcd} - (4-D)\alpha J_{abcd}) + iP_{abcd,ij}(\partial J_{abcd}^{ij} - (2-d)\alpha J_{abcd}^{ij}) \right\} \\ & + \frac{1}{4} \int d\mathbf{x}d\mathbf{y}dz \left\{ \alpha s_a(\mathbf{x})G'(\mathbf{x}-\mathbf{y})s_a(\mathbf{y}) \right\}, \end{aligned} \quad (5.20)$$

with

$$\begin{aligned} s_a = & \left[iJ_a + 2P_b J_{ab} - 2\partial_j(J_{ab}^{ij}\partial_i P_b) + 3P_{bc}J_{abc} - \partial_j(J_{abc}^{ij}\partial_i P_{bc}) \right. \\ & \left. + P_{bc,ij}J_{abc}^{ij} + 4P_{bcd}J_{abcd} - \frac{2}{3}\partial_j(J_{abcd}^{ij}\partial_i P_{bcd}) + 2J_{abcd}^{ij}P_{bcd,ij} \right], \end{aligned} \quad (5.21)$$

$G'(\mathbf{x}) \equiv M\partial_M G_M(\mathbf{x})$, and $\partial = \frac{\partial}{\partial z} - \alpha \sum_{i=1}^D x_i \frac{\partial}{\partial x_i}$. Here $\int d\mathbf{x}$ and $\int d\mathbf{y}$ are integrations on a D -dimensional manifold \mathcal{M}^D , and $G_M^{-1}(\mathbf{x})$ is the regularized kinetic energy with cut-off M .

The dual theory is given by the functional integrals of the source fields J and their conjugate fields P in the $(D+1)$ -dimensional space $\mathcal{M}^D \times [0, \infty)$ with the boundary condition $J(\mathbf{x}, z=0) = \mathcal{J}(\mathbf{x})$. If the D -dimensional manifold \mathcal{M}^D has a finite volume V , the volume at scale z is given by $Ve^{-\alpha Dz}$.

One key difference from the 0-dimensional theory is that there exist bulk fields with non-trivial spins. In Eq. (5.20), there are spin two fields which are coupled to the energy momentum tensor at the boundary. In the presence of more general deformations in the boundary theory, one needs to introduce fields with higher spins [80, 81].

One can decompose the tensor sources into singlets and traceless parts and take the large N limit where saddle point solutions become exact for singlet fields. One can integrate out all non-singlet fields and obtain an effective theory for single fields alone. However, the resulting effective action for single fields become non-local in this $O(N)$ vector model. This is because there are light non-singlet fields in the bulk and integrating over those soft modes generates non-local correlations for singlet fields. This means that we should keep light non-singlet fields as ‘low energy degrees of freedom’ in the bulk description if we want to use a local description.

5.3 Phase Transition and Critical Behaviors

One can understand the phase transition and the critical properties of the model in $D > 2$ using the holographic theory. As one tunes the singlet sources at the UV boundary, the shape of potential in the IR limit changes accordingly. In some parameter regime, the bulk fields are forced to spontaneously break the $O(N)$ symmetry. This is illustrated in Fig. 11.

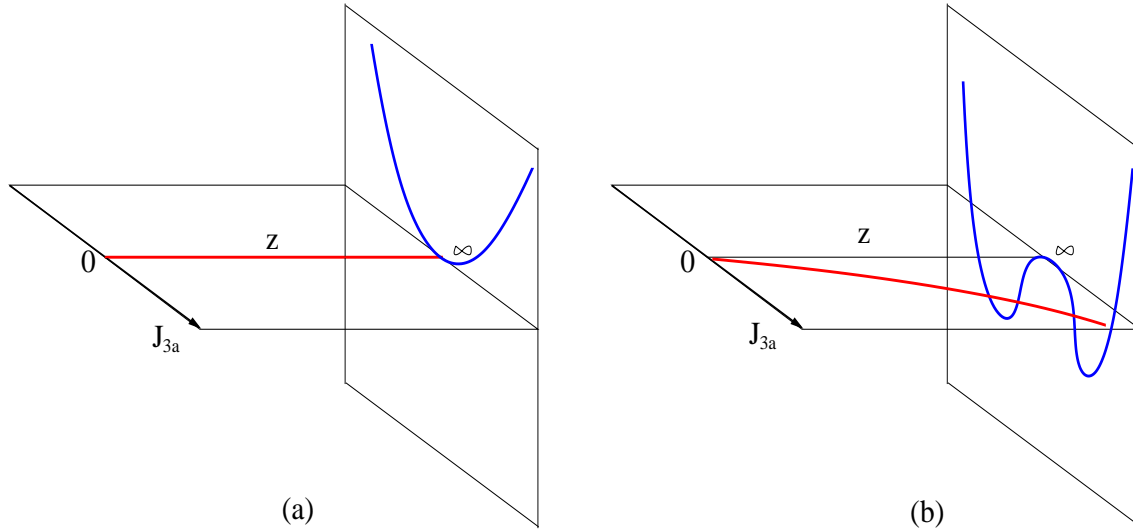


Figure 11: Saddle point configuration for a non-singlet source field $J_{3a}(z)$ (a) in the disordered phase and (b) in the ordered phase. When \mathcal{J}_2 is sufficiently negative, a Mexican-hat potential at the IR boundary drags $J_{3a}(z)$ away from $J_{3a}(z) = 0$ in the bulk. At the critical point, J_{3a} at the IR boundary $z = \infty$ is more or less free to fluctuate, generating algebraic correlations between fields inserted at the UV boundary $z = 0$.

One can also compute correlation functions of the singlet operators at the critical point using the similar method used in the AdS/CFT correspondence. For this one integrates over all bulk fields consistent with the x -dependent UV boundary condition. The bulk action can be computed as a function of the UV sources and this gives the generating function for the boundary theory. From this one can compute the critical exponents of singlet operators, which matches with the known field theory predictions. More recently, the present prescription has been applied to large N gauge theory where a field theory of closed loops arise as a holographic dual for the $U(N)$ gauge theory [82].

6 Acknowledgment

This note is based on the lectures given at TASI in June 2010. I would like to thank Thomas Banks, Michael Dine and Subir Sachdev for their kind invitation to give lectures at TASI. I am also grateful to Thomas DeGrand, K.T. Mahanthappa and Susan Spika for the hospitality during the summer school. Parts of this material were also presented at the APCTP Focus Program on Aspects of Holography and Gauge/string duality held at Pohang, Korea in August 2010. I thank Deog Ki Hong, Sang-Jin Sin and Piljin Yi for giving me the opportunity to give lectures. I would like to thank lecturers, participants and students of TASI and APCTP workshop for stimulating comments and discussions. Finally, I thank Andrey Chubukov, Guido Festuccia, Matthew Fisher, Sean Hartnoll, Michael Hermele, Yong Baek Kim, Patrick Lee, Hong Liu, Max Metlitski, Lesik Motrunich, Joe Polchinski, Subir Sachdev, T. Senthil, Mithat Unsal and Xiao-Gang Wen for many illuminating discussions in the past. This work was supported by NSERC.

References

- [1] X.-G. Wen, *Quantum Field Theory of Many-body Systems: From the Origin of Sound to an Origin of Light and Electrons* (Oxford Graduate Texts).
- [2] S. Sachdev, *Quantum Phase Transitions*, Cambridge University Press.
- [3] D. Friedan, Z. Qui and S. Shenkar, Phys. Lett. B **151**, 37 (1985).
- [4] S. Thomas, *Emergent Supersymmetry*, KITP talk (2005).
- [5] D. B. Kaplan, Phys. Lett. B **136**, 162 (1984).
- [6] P. Fendley, K. Schoutens and J. de Boer, Phys. Rev. Lett. **90**, 120402 (2003).
- [7] P. Fendley, B. Nienhuis and K. Schoutens, J. Phys. A **36**, 12399 (2003).
- [8] S. Catterall, D. B. Kaplan and Mithat Unsal, arXiv: 0903.4881.
- [9] S.-S. Lee, Phys. Rev. B **76**, 075103 (2007).
- [10] Y. Yu and K. Yang, arXiv:1005.1399.
- [11] L. Balents, M. P. A. Fisher and C. Nayak, Int. J. Mod. Phys. B **12**, 1033 (1998).
- [12] P. W. Anderson, Science **235**, 1196 (1987); P. Fazekas and P. W. Anderson, Philos. Mag. **30**, 432 (1974).
- [13] A. Y. Kitaev, Ann. Phys. (N.Y.) **303**, 2 (2003).
- [14] X.-G. Wen, Phys. Rev. Lett. **90**, 016803 (2003).
- [15] R. Moessner and S. L. Sondhi, Phys. Rev. Lett. **86**, 1881 (2001).
- [16] X.-G. Wen, Phys. Rev. Lett. **88**, 11602 (2002).
- [17] X.-G. Wen, Phys. Rev. B **68**, 115413 (2003).
- [18] O. I. Motrunich and T. Senthil, Phys. Rev. Lett. **89**, 277004 (2002).
- [19] O. I. Motrunich and T. Senthil, Phys. Rev. B **71**, 125102 (2005).
- [20] S.-S. Lee and P. A. Lee, Phys. Rev. B **72**, 235104 (2005).
- [21] A. M. Polyakov, Phys. Lett. B **59**, 82 (1975); Nucl.Phys. B **120**, 429 (1977).
- [22] T. Senthil, A. Vishwanath, L. Balents, S. Sachdev and M. P. A. Fisher, Science **303** 1490 (2004).
- [23] M. A. Levin and X.-G. Wen Phys. Rev. B **67**, 245316 (2003); *ibid.* **71**, 045110 (2005).
- [24] For more comprehensive reviews, see P. A. Lee, N. Nagaosa and X.-G. Wen, Rev. Mod. Phys. **78**, 17 (2006); S. Sachdev, arXiv:0901.4103; L. Balents, Nature **464**, 199 (2010).

- [25] M. B. Hastings, Phys.Rev. B **69**, 104431 (2004).
- [26] X.-G. Wen, Phys. Rev. B **65**, 165113 (2002).
- [27] O. I. Motrunich, Phys. Rev. B **72**, 045105 (2005).
- [28] S.-S. Lee and P. A. Lee, Phys. Rev. Lett. **95**, 036403 (2005).
- [29] X.-G. Wen, F. Wilczek and A. Zee, Phys. Rev. B **39**, 11413 (1989).
- [30] N. Read and S. Sachdev, Phys. Rev. Lett. **66**, 1773 (1991).
- [31] T. Senthil and M. P. A. Fisher, Phys. Rev. B **62**, 7850 (2000).
- [32] L. B. Ioffe and A. I. Larkin, Phys. Rev. B **39**, 8988 (1989).
- [33] G. Murthy and S. Sachdev, Nucl. Phys. B **344**, 557 (1990).
- [34] V. Borokhov, A. Kapustin and X. Wu, J. High Ener. Phys. **0212** 044 (2002).
- [35] M. A. Metlitski, M. Hermele, T. Senthil, M. P. A. Fisher, Phys. Rev. B **78**, 214418 (2008).
- [36] M. Hermele, T. Senthil, M. P. A. Fisher, P. A. Lee, N. Nagaosa and X.-G. Wen, Phys. Rev. B **70**, 214437 (2004).
- [37] S.-S. Lee, Phys. Rev. B **78**, 085129 (2008).
- [38] R. Shankar, Rev. Mod. Phys. **66**, 129 (1994).
- [39] S.-W. Tsai, A. H. Castro Neto, R. Shankar, and D. K. Campbell, Phys. Rev. B **72**, 054531 (2005).
- [40] P. A. Lee, Phys. Rev. Lett. **63**, 680 (1989).
- [41] B. I. Halperin, P. A. Lee, and N. Read, Phys. Rev. B **47**, 7312 (1993).
- [42] P. A. Lee and N. Nagaosa, Phys. Rev. B **46** 5621 (1992).
- [43] J. Polchinski, Nucl. Phys. B **422**, 617 (1994).
- [44] Y. B. Kim, A. Furusaki, X.-G. Wen and P. A. Lee, Phys. Rev. B **50**, 17917 (1994).
- [45] C. Nayak and F. Wilczek, Nucl. Phys. B **417**, 359 (1994); **430**, 534 (1994).
- [46] B. L. Altshuler, L. B. Ioffe and A. J. Millis, Phys. Rev. B **50**, 14048 (1994).
- [47] O. I. Motrunich and M. P. A. Fisher, Phys. Rev. B **75**, 235116 (2007).
- [48] S.-S. Lee, Phys. Rev. B **80**, 165102 (2009).
- [49] M. Metlitski and S. Sachdev, arxiv:1001.1153.

- [50] V. Oganesyan, S. A. Kivelson, and E. Fradkin, Phys. Rev. B **64**, 195109 (2001).
- [51] W. Metzner, D. Rohe, and S. Andergassen, Phys. Rev. Lett. **91**, 066402 (2003).
- [52] V. M. Galitski, G. Refael, M. P. A. Fisher, and T. Senthil, Phys. Rev. Lett. **95**, 077002 (2005).
- [53] M. J. Lawler, V. Fernandez, D. G. Barci, E. Fradkin, L. Oxman, Phys. Rev. B **73**, 085101 (2006).
- [54] R. K. Kaul, A. Kolezhuk, M. Levin, S. Sachdev, and T. Senthil, Phys. Rev. B **75**, 235122 (2007).
- [55] R.K. Kaul, Y.B. Kim, S. Sachdev, T. Senthil, Nat. Phys. **4**, 28 (2008).
- [56] J. Rech, C. Pepin, and A. V. Chubukov, Phys. Rev. B **74**, 195126 (2006).
- [57] T. Senthil, Phys. Rev. B **78**, 035103 (2008).
- [58] D. L. Maslov and A. V. Chubukov, Phys. Rev. B **81**, 045110 (2010).
- [59] D. F. Mross, J. McGreevy, H. Liu and T. Senthil, arXiv:1003.0894.
- [60] S.-J. Rey, Prog. Theor. Phys. Supp. **177**, 128 (2009).
- [61] S.-S. Lee, Phys. Rev. D **79**, 086006 (2009).
- [62] H. Liu, J. McGreevy and D. Vegh, arXiv:0903.2477.
- [63] M. Cubrovic, J. Zaanen and K. Schalm, Science **325**, 439 (2009).
- [64] T. Faulkner, H. Liu, J. McGreevy and D. Vegh, arXiv:0907.2694.
- [65] F. Denef, S. A. Hartnoll, and S. Sachdev, Phys. Rev. D **80**, 126016 (2009).
- [66] S. A. Hartnoll, J. Polchinski, E. Silverstein and D. Tong, J. High Ener. Phys. **1004**, 120 (2010).
- [67] T. Faulkner, N. Iqbal, H. Liu, J. McGreevy and D. Vegh, arXiv:1003.1728.
- [68] T. Faulkner and J. Polchinski, arXiv:1001.5049.
- [69] F. Larsen, and G. van Anders, arXiv:1006.1846.
- [70] S. Sachdev, arXiv:1006.3794.
- [71] I.R. Klebanov and A.M. Polyakov, Phys. Lett. B **550**, 213 (2002).
- [72] S. R. Das and A. Jevicki, Phys. Rev. D **68**, 044011 (2003).
- [73] R. Gopakumar, Phys. Rev. D **70**, 025009 (2004); *ibid.* **70**, 025010 (2004).

- [74] I. Heemskerk, J. Penedones, J. Polchinski and J. Sully, *J. High Energy Phys.* **10**, 079 (2009).
- [75] S.-S. Lee, *Nucl. Phys. B* **832**, 567 (2010).
- [76] J. Polonyi, arXiv:hep-th/0110026v2.
- [77] J. Polchinski, *Nucl. Phys. B* **231**, 269 (1984).
- [78] J. de Boer, E. Verlinde and H. Verlinde, *J. High Energy Phys.* **08**, 003 (2000).
- [79] R. Arnowitt, S. Deser, and C. Misner, *Phys. Rev.* **116**, 1322 (1959).
- [80] M. A. Vasiliev, arXiv:hep-th/9910096.
- [81] S. Giombi and Xi Yin, arXiv:0912.3462.
- [82] S.-S. Lee, arXiv:1011.1474.